

Nikita P. Zelensky · Jean-Paul Berthias  
Frank G. Lemoine

## DORIS time bias estimated using Jason-1, TOPEX/Poseidon and ENVISAT orbits

Received: 18 January 2006 / Accepted: 1 June 2006 / Published online: 26 July 2006  
© Springer-Verlag 2006

**Abstract** DORIS is a globally distributed, all-weather satellite tracking system providing near-continuous precise Doppler coverage of the TOPEX/Poseidon (T/P), Jason-1, ENVISAT, and SPOT series of satellites. The DORIS system, which has been critical in establishing the high-precision orbit determination standards now enjoyed by these missions, continues to evolve and improve. There is a small, 5 to 10  $\mu$ s, discrepancy between the DORIS time-tag computed by Centre National d'Etudes Spatiales (CNES) using the DORIS timing data, and a time-tag estimated using DORIS range-rate data with respect to orbits referred to Satellite Laser Ranging (SLR) or Global Positioning System (GPS) time. This discrepancy is evaluated using DORIS time biases estimated over T/P, Jason-1, and ENVISAT orbits, which are computed using SLR or GPS tracking and reference SLR or GPS time. Although DORIS is installed on other satellites, these are the only three where the DORIS time bias can be observed with the help of an alternate tracking system – SLR or GPS. For T/P, Jason-1 and ENVISAT, this DORIS time bias quantities to 5–10  $\mu$ s. Over the span of the T/P mission following cycle 92, this time bias has ranged from +10 to –10  $\mu$ s. This paper addresses the precision and nature of the estimated time biases by evaluating such estimates

over orbits computed with various gravity field models, computed using SLR + DORIS and GPS tracking, and computed by the Goddard Space Flight Center (GSFC), Jet Propulsion Laboratory (JPL), and CNES analysis centers. The paper includes descriptions of the DORIS measurement, time-tag processing, expected time-tag error, and time bias estimation. In describing the estimated DORIS time bias, the paper offers a new approach for evaluating the DORIS resolution capability.

**Keywords** DORIS · Precise orbit determination (POD) · Time-tag error · TOPEX/Poseidon (T/P) · Jason-1 · ENVISAT · SLR · GPS · IDS

### 1 Introduction

DORIS offers an accurate all-weather near-global Doppler satellite tracking capability. In its present form, the DORIS has achieved 2-cm radial orbit precision for both TOPEX/Poseidon (T/P) (Nouel et al. 1994; Marshall et al. 1995) and Jason-1 (Menard et al. 2003) satellites. The latest generation of DORIS receivers promise even further improvement to the tracking capability, offering additional channels and the possibility of integrated carrier-phase observations (Tavernier et al. 2003).

With more than 50 permanent, globally distributed beacons, currently tracking five satellites, the DORIS is also an important contributor to the realization and maintenance of the International Terrestrial Reference System (ITRS; Tavernier et al. 2005). Applications include the recovery of DORIS station positions and velocities (Willis and Ries 2005), Earth orientation parameters (EOPs), and geocenter variations (Willis et al. 2005a).

There is a small, 5 to 10  $\mu$ s, discrepancy between the DORIS time-tag computed by Centre National d'Etudes Spatiales (CNES) using the DORIS timing data, and a time-tag estimated using DORIS range-rate data with respect to orbits based on Satellite Laser Ranging (SLR) or Global Positioning System (GPS) tracking, and thereby referencing SLR or

---

N. P. Zelensky (✉)  
SGT Inc., 7701 Greenbelt Road, Greenbelt,  
MD 20770, USA  
E-mail: nzelenky@sgt-inc.com  
Tel.: +33-5-61283236  
Fax: +33-5-61281748

J.-P. Berthias  
Centre National d'Etudes Spatiales, 18 avenue Edouard Belin,  
31401 Toulouse Cedex, France  
E-mail: jean-paul.berthias@cnes.fr  
Tel.: +33-5-61283236  
Fax: +33-5-61281748

F. G. Lemoine  
NASA Goddard Space Flight Center, Planetary Geodynamics,  
Code 698, Greenbelt, MD 20771, USA  
E-mail: Frank.Lemoine@gsfc.nasa.gov  
Tel.: +1-301-6146109  
Fax: +1-301-6146099

GPS time. Given the high degree of accuracy expected in the DORIS, the SLR and GPS time systems, the presence of such a discrepancy remains a conundrum. In this paper, this discrepancy will be referred to as the DORIS time bias. Although, as shown in this analysis, the effect of such a time bias on precise orbit determination (POD) is small; it may not be negligible for geodetic parameter recovery.

This study evaluates Jason-1 and T/P time biases over orbits produced at different Analysis Centers (ACs) and produced using GPS and SLR + DORIS tracking, as well as over different time-scales. An evaluation of the DORIS time bias for ENVISAT is also included. In describing the non-zero time bias estimate, the paper offers a new approach for evaluating the DORIS resolution capability.

## 2 DORIS measurement and time tag

The dual-frequency signal emitted from the ground-based DORIS beacon is received by the on-board DORIS package and recorded at both frequencies as an integrated Doppler count measurement. Thanks in large measure to the quality of the measurement performed by the DORIS receiver and to the ultra-stable oscillators (USO) present in the beacon and in the on-board package; the DORIS measurements are of high accuracy, showing a precision of 0.3–0.5 mm/s (Brunet et al. 1995, Escudier et al. 1998). The measurements are temporarily stored on-board the satellite and periodically transferred down with the telemetry stream to the CNES Mission Center in Toulouse, France.

On the ground, the DORIS measurements are processed by the CNES Mission Center to clean-up the data and to transform the instrument time to International Atomic Time (TAI). The Doppler measurements are converted to a range-rate measurement in units of velocity and include an ionosphere correction computed from the dual-frequency measurement. The resultant DORIS data are then distributed to the two IDS (International DORIS Service) Data Centers: CDDIS (Crustal Dynamics Data Information System) and IGN (Institut Géographique National) (Berthias 2002; Tavernier et al. 2005). The final DORIS range-rate measurement can be expressed:

$$\begin{aligned} \text{DRR}(T) &= \frac{c}{f'_{\text{beacon}}} \left[ \frac{D}{T_2 - T_1} - (f'_{\text{beacon}} - f'_{\text{satellite}}) \right] \\ &= \frac{c}{f'_{\text{beacon}}} \left[ -\frac{f_{\text{beacon}}(\tau_2 - \tau_1)}{T_2 - T_1} - (f_{\text{satellite}} - f'_{\text{satellite}}) \right. \\ &\quad \left. + (f_{\text{beacon}} - f'_{\text{beacon}}) \right] \end{aligned} \quad (1)$$

where

DRR = DORIS range-rate measurement

$T$  = TAI time-tag corresponding to start of count interval (equal to  $T_1$ )

$D$  = integrated Doppler count between  $T_1$  and  $T_2$

$f_{\text{beacon}}$  = actual frequency transmitted by the beacon

$f_{\text{satellite}}$  = actual frequency generated by the on-board receiver

$f'_{\text{beacon}}$  = nominal frequency transmitted by the beacon

$f'_{\text{satellite}}$  = CNES best estimate of frequency generated by on-board receiver

$T_1, T_2$  = beginning and end times of the count interval in TAI

$\tau_1, \tau_2$  = total ground-satellite propagation delay times at the beginning and end epochs of the count interval.

$c$  = speed of light

In processing the DORIS data for POD or geodetic applications, the quantity  $\tau_2 - \tau_1$  (which can be converted to a differenced range) provides the satellite tracking information, whereas  $((f_{\text{beacon}} - f'_{\text{beacon}}) - (f_{\text{satellite}} - f'_{\text{satellite}}))$  is an unknown residual frequency bias estimated with each pass of DORIS data in the orbit solution, and removed. The count interval duration,  $T_2 - T_1$ , typically 10 s, is provided with the DORIS data.

The DORIS time reference is delivered by caesium clocks linked to TAI and connected to the two master DORIS beacons, one in Toulouse and the other in Kourou (a third master beacon has recently, in September 2005, been added in Hartebeesthoek). The DORIS integrated Doppler measurements created on-board from all ground beacons are initially time-tagged using the DORIS internal clock and periodically transmitted to the CNES Mission Center. Low-resolution DORIS single-frequency pseudorange tracking data are also collected by the receiver and processed daily at the CNES using a predicted orbit to determine the relationship between TAI and satellite clock time using a third-order polynomial. Third-generation DORIS beacons actually transmit the synchronization signal on both frequencies; however, only one of the two pseudorange measurements is included in the telemetry.

The pseudorange observation is the difference between satellite receiving time and beacon transmit time of a synchronization bit contained in the beacon message. For the master beacons, the transmit time is precisely known in TAI. Thus, in addition to propagation delay, the pseudorange measurement contains the difference between satellite time and TAI. Satellite clock time is corrected to TAI using a third-order polynomial estimated over an approximately 10-day period with the pseudorange data.

$$T = t + a_0 + a_1(t - t_0) + a_2(t - t_0)^2 + a_3(t - t_0)^3 \quad (2)$$

where

$T$  = final DORIS time tag (TAI start of count interval)

$t$  = initial DORIS time tag (satellite clock start of count interval)

$t_0$  = arbitrary time close to start of 10-day cycle span (satellite clock time)

$a_0$  = estimated satellite clock offset with estimate error  $\delta a_0$ .

$a_1$  = estimated satellite clock drift correction including the relativistic clock frequency offset term with estimate error  $\delta a_1$ .

$a_2$  = estimated satellite clock drift-rate correction with estimate error  $\delta a_2$ .

$a_3$  = estimated satellite clock acceleration-rate correction with estimate error  $\delta a_3$ .

Refinement of the polynomial clock correction (Eq. 2) is iterative – with each new set of improved time-tags, the re-edited DORIS Doppler data are used to improve the orbit, which is then used in a new timing solution. Convergence is reached quickly, typically with two iterations; the precision of the pseudorange data is limited to the microsecond level (equivalent to  $\sim 300$  m), so that any orbit model of meter precision is enough to pin-point the time-tags with sufficient precision. Pseudorange data are not provided to the user community, as no further application of the 300-m precision data can improve either the orbit or the TAI time estimate.

In practice, the uniterated timing solution is used for orbit deliveries with a latency of 1 day, and the iterated solution spanning one orbit cycle is used for POD and delivery. The timing solution spanning one orbit cycle does not exhibit breaks at day boundaries. The derivative of this timing polynomial (Eq. 2) gives the on-board frequency estimate  $f'_{\text{satellite}}$ , used in Eq. (1) to convert Doppler count to range-rate.

This study evaluates remaining error in  $T$  by estimating a constant time bias with respect to orbits computed using SLR or GPS data and thereby referencing the SLR or GPS time systems. Assuming negligible error in the master station caesium clocks and GPS or SLR time (see Sect. 3), the estimated DORIS time-tag bias, can be expressed:

$$\delta\check{T} = \delta T_{\text{polynomial}} + \delta T_{\text{orbit}} + \delta T_{\text{noise}} + \delta T_{\text{unknown}} \quad (3)$$

where

$\delta\check{T}$  = estimated DORIS time bias

$\delta T_{\text{polynomial}}$  = error in TAI time-tag polynomial model estimate (Eq. 2)

$\delta T_{\text{orbit}}$  = error in orbit used to estimate time bias

$\delta T_{\text{noise}}$  = precision of the DORIS time bias estimate

$\delta T_{\text{unknown}}$  = error of unknown origin

and

$$\delta T_{\text{polynomial}} \approx \delta a_0 + \delta a_1 \Delta T + \delta a_2 \Delta T^2 + \delta a_3 \Delta T^3 \\ + (\text{effect of un-modeled higher order terms}) \quad (4)$$

where

$\delta T_{\text{polynomial}}$  = error in TAI time tag polynomial model estimate

$\Delta T$  = arc time span, normally 10-days for Jason and T/P

$\delta a_0$  = error clock polynomial offset term

$\delta a_1$  = error clock polynomial drift term

$\delta a_2$  = error clock polynomial drift-rate term

$\delta a_3$  = error clock polynomial acceleration-rate term

The term  $\delta T_{\text{polynomial}}$  in Eqs. (2) and (4) reflects errors of commission and omission in modeling the DORIS satellite clock (Eq. 2). These include error in the estimated clock polynomial terms, effects of short-term instability in the on-board receiver and ground beacons, and other possible error in the measurement of the on-board receiver's transit time.

In estimating the DORIS time-tag (Eq. 2), the precision of the pseudorange data will contribute only  $1 \mu\text{s}$  to the  $\delta T_{\text{polynomial}}$  error component. However, should  $\delta T_{\text{polynomial}}$

dominate  $\delta\check{T}$ , the DORIS time bias estimated for different satellites should vary between the satellites, as it would largely pertain to error in the estimation of the on-board clock behavior, and would not be due to some common source of error. Estimates of  $\delta\check{T}$  over intervals shorter than 10 days may shed light on the relative magnitude of the estimated polynomial error terms,  $\delta a_1$ ,  $\delta a_2$ , and  $\delta a_3$ , and possible presence of shorter-term (under 10-day) instability in the DORIS satellite clock.

Short-period effects exist in the relation between on-board time and TAI. These include a periodic relativistic correction due to orbit eccentricity, and a local clock drift induced by frequency variations when crossing the South Atlantic Anomaly (SAA) region (Willis et al. 2004; Lemoine and Capdeville 2006). These effects are negligible compared to the  $1 \mu\text{s}$  uncertainty introduced by the pseudorange data precision and are not included in modeling the time-tag (Eq. 2). For example, considering the standard expression of the periodic relativistic term (McCarthy and Petit 2003), the maximum contribution is under 1 ns for a satellite at T/P altitude with the T/P eccentricity of 0.0005. Similarly, the frequency variations induced by the SAA occur over such short periods that even for very sensitive USO s such as the one on Jason-1, the integrated impact on on-board time should not exceed a microsecond over 10 days (F. Mercier, private communication).

### 3 SLR and GPS measurement time-tag

Currently there are about 50 active SLR stations world-wide. Although individual SLR station clocks vary from crystal oscillators to hydrogen masers, all qualified sites employ GPS receivers to steer station time to UTC (Coordinated Universal Time) with an accuracy of better than  $0.1 \mu\text{s}$ , as provided by the International Laser Ranging Service (ILRS) (Pearlman et al. 2002) at [http://ilrs.gsfc.nasa.gov/engineering\\_technology/timing/oscillators.html](http://ilrs.gsfc.nasa.gov/engineering_technology/timing/oscillators.html).

The GPS time is given by its Composite Clock, which is a Kalman-filtered ensemble of clock times, and information from the several ground monitor stations and all operational GPS satellites. Each GPS satellite carries two rubidium and two caesium clocks (e.g. Hutsell et al. 2002). The U.S. Naval Observatory, which maintains UTC(USNO) time and monitors GPS time (which is steered to UTC(USNO)), finds the RMS difference between the two to be well under 50 ns (<ftp://tycho.usno.navy.mil/pub/gps/gpstt.txt>).

### 4 Time bias estimation

In the Goddard Space Flight Center (GSFC) SLR+DORIS orbit solution strategy for Jason, T/P, and ENVISAT, typically the DORIS frequency, troposphere biases per pass and one-time bias per arc are estimated simultaneously with the orbit over the arc [typically 10 days for Jason and T/P (Luthcke et al. 2003), and 7 days for ENVISAT]. The DORIS time is

**Table 1** DORIS time bias test solution strategy

| Model/parameter      | Description  |
|----------------------|--|
| Assumed models       | <ul style="list-style-type: none"> <li>● Specified 10-day test orbit</li> <li>● ITRF2000 reference frame (Altamimi et al. 2002; Willis et al. 2005a)</li> </ul>                        |
| Estimated parameters | <ul style="list-style-type: none"> <li>● DORIS measurement bias per pass</li> <li>● DORIS troposphere scale per pass</li> <li>● DORIS time bias per 10 days or as specified</li> </ul> |

thus shifted by a constant to align it with the SLR network time.

In an additional secondary approach, the DORIS time bias is estimated by holding a previously selected estimated orbit fixed, and processing the available DORIS tracking data solving for frequency, troposphere biases per pass, and one time bias per arc (Table 1). Such an approach determines a time bias identical to the one computed during orbit determination. However, this approach also offers the possibility for estimating a time bias using an orbit computed without DORIS or computed at a different AC such as the Jet Propulsion Laboratory (JPL) or CNES.

The GSFC least-squares orbit determination batch processor GEODYN (Pavlis 2006) is used for both modes of analysis. We note that one factor facilitating these analyses of the DORIS timing bias, is that for TOPEX and Jason-1, the orbits computed via different geodetic techniques or by the ACs differ by only 1–3 cm in the radial component, and 10–20 cm along-track and cross-track (Luthcke et al. 2003; Haines et al. 2004). The orbits selected for this analysis all observe the same definition of the International Terrestrial Reference Frame ITRF2000 (Altamimi et al. 2002), and as will be shown (Sects. 5 and 6), the effect of any possible inconsistency in the reference frame realization between these orbits is no larger than the level of the precision of the time bias estimate.

The GEODYN partial used for estimating the time bias is simply constructed from a first-order truncation of the Taylor expansion of  $DRR(T + \delta T)$ , where DRR is the computed DORIS range-rate measurement,  $T$  is the time tag and  $\delta T$  is the time tag error (Pavlis 2006). The DORIS measurement is modeled using the computed orbit and computed DORIS station position.

The DORIS time bias is estimated using the ground beacon to satellite range difference information of the DORIS measurement (Eq. 1), which should be most sensitive to the along-track orbit component. The effect of a positive time-tag shift on an orbit determined with only DORIS is seen largely as a positive shift in the along-track position, moving the orbit further along its trajectory in time.

In the GEODYN sign convention, the time bias  $\delta T$  is subtracted from the time tag  $T$ , so for example, a time bias of  $+6\mu\text{s}$  applied in GEODYN would place T/P 4cm behind the true along-track position. To evaluate this effect, several DORIS-only T/P and Jason orbit solutions were made perturbing the time bias and comparing the orbits to a “truth” orbit solution with zero time bias (Table 2).

**Table 2** DORIS-only orbit sensitivity to time bias error with GEODYN

| Time bias $\delta T$ ( $\mu\text{s}$ )<br>(Error–Truth) | DORIS RMS<br>residuals (mm/s) | Error – Truth orbit<br>difference (cm) |                 |                     |
|---|-------------------------------|--|-----------------|---------------------|
|   |                               | Radial<br>RMS                          | 3D total<br>RMS | Along-track<br>Mean |
| TOPEX (cycle 344)                                       |                               |  |                 |                     |
| 0   | 0.472                         | –                                      | –               | –                   |
| –6  | 0.472                         | 0.001                                  | 4.174           | +4.168              |
| –10   | 0.472                         | 0.002                                  | 6.970           | +6.960              |
| –60   | 0.472                         | 0.010                                  | 41.791          | +41.774             |
| Jason (cycle 001)                                       |                               |  |                 |                     |
| 0   | 0.391                         | –                                      | –               | –                   |
| –6  | 0.391                         | 0.001                                  | 4.184           | +4.178              |
| –10   | 0.391                         | 0.002                                  | 6.977           | +6.968              |
| –60   | 0.391                         | 0.010                                  | 41.804          | +41.747             |

**Table 3** Mean along-track error versus DORIS time bias regression statistics

| Satellite | Data<br>points | Intercept (cm) |       | Slope (cm/ $\mu\text{s}$ ) |         | Correlation<br>coefficient | RMS<br>fit (cm) |
|-----------|----------------|----------------|-------|----------------------------|---------|----------------------------|-----------------|
|           |                | Estimate       | Error | Estimate                   | Error   |                            |                 |
| TOPEX     | 10             | 0.002          | 0.002 | –0.69573                   | 0.00004 | 1.000                      | 0.0046          |
| Jason     | 10             | –0.003         | 0.001 | –0.69575                   | 0.00002 | 1.000                      | 0.0030          |

From the simple Jason and TOPEX test results (Table 2), a strong linear relationship is seen to exist between small, microsecond-level perturbations in the time bias and shifts in the resulting along-track orbit component (Table 3). As expected, the estimated intercept is zero, and the slope corresponds to the mean Earth-fixed orbit velocity.

## 5 Jason DORIS time bias/orbit resolution precision

In this study, the DORIS measurement is modeled using a previously computed orbit held fixed and the DORIS ITRF2000 station complement DPOD2000 (Willis and Ries 2005). Table 4 offers a summary of the orbits used in the study. Even though GSFC Jason DORIS processing does not include any special treatment for the effect of the SAA, it does not appear that the estimated time biases are sensitive to this effect (Sect. 6), and so analysis using this time bias series need not consider possible contamination due to the SAA.

By estimating a time bias with the orbit held fixed, the DORIS data uses the computed orbit to best shift the DORIS observation time-tag. The question is posed: (1) “how well can DORIS resolve the time bias?”. Posing question (1) is directly related to asking (2) “how well can DORIS resolve the along-track orbit position?”.

No direct method for evaluating DORIS resolution to microsecond accuracy is evident. Although 1-cm radial accuracy has been achieved for the Jason GPS-based orbits (Luthcke et al. 2003; Haines et al. 2004), differences between the best orbits suggest 10-day mean along-track orbit errors can range 3 to 6 mm. This level of error may be too large for such an orbit to be used as an absolute reference. A relative measure for evaluating the DORIS ability to resolve the time bias is presented subsequently.

**Table 4** Orbit summary

| Satellite     | Center | Orbit Name    | Description  |
|---------------|--------|---------------|--|
| Jason (JA)    | GSFC   | SLR+DORIS     | SLR+DORIS JGM-3/ITRF2000 dynamic orbit, estimate DORIS time bias (Luthcke et al. 2003) |
|               |        | test_no_tbias | SLR+DORIS JGM-3/ITRF2000 dynamic orbit, POD strategy similar to one employed at CNES   |
|               |        | DORIS-only    | DORIS JGM-3/ITRF2000 dynamic orbit   |
|               |        | GPS           | GPS JGM-3/ITRF2000 reduced-dynamic orbit (Luthcke et al. 2003)                         |
|               |        | GPS+SLR       | GPS+SLR JGM-3/ITRF2000 reduced-dynamic orbit (Luthcke et al. 2003)                     |
| TOPEX (T/P)   | JPL    | JPL           | GPS JGM-3 reduced-dynamic orbit (Haines et al. 2003)                                   |
|               | CNES   | CNES          | SLR+DORIS JGM-3/ITRF2000 dynamic orbit (Nouel et al. 1994)                             |
| TOPEX (T/P)   | GSFC   | JGM3          | SLR+DORIS JGM-3 dynamic orbit, estimate DORIS time bias (Marshall et al. 1995)         |
|               |        | GGM02C        | SLR+DORIS GGM02C/ITRF2000 dynamic orbit, estimate DORIS time bias                      |
| ENVISAT (ENV) | GSFC   | ENV           | SLR+DORIS GGM01C/ITRF2000 dynamic orbit (nominal 7-day arc), estimate DORIS time bias  |

Jason-1 carries three precise tracking systems on-board: DORIS, SLR, and GPS. Figure 1 shows time biases estimated for four types of Jason GSFC orbit solutions: SLR+DORIS, GPS-only, GPS+SLR, and a DORIS-only solution to sanity-check our test methodology. As expected the DORIS-only time biases are close to zero (average of  $0.004\mu\text{s} \pm 0.117\mu\text{s}$ ), illustrating the consistency of the analysis. The timing and frequency standards used by SLR are disciplined by GPS so that, in principle, the SLR and GPS data and derived orbits should refer to the same time standard.

The SLR+DORIS and GPS-based orbit time bias estimates are very close (0.85 correlation). Differences between these time bias estimates can be explained by orbit error (Sect. 6). Table 3 has shown that a linear model very accurately explains the relationship between time bias differences and mean along-track orbit differences. Since the time biases were estimated in solutions with the orbits held fixed, the SLR+DORIS/GPS orbit differences can be considered as the dependent variable in evaluating the linear relationship to the respective time bias differences. The degree to which these quantities fit a linear model should reflect the DORIS capability for resolving a time bias.

Indeed, the time bias differences show a robust linear fit to the mean along-track differences (Fig. 2) with a correlation coefficient of 0.96 (Table 5). The linear regression estimates make physical sense as well – the estimated zero-intercept (Table 5) confirms there is no time offset between the GPS and SLR systems to  $0.1\mu\text{s}$ , and the estimated slope corresponds, within the margin of error, to the mean orbital velocity. The sign of the corresponding slope is consistent with that of the slope estimated in Table 3. The RMS scatter about the straight-line fit suggests the DORIS time bias is estimated with a relative accuracy of  $0.345\mu\text{s}$  over 10-days, and conversely that the DORIS can resolve the 10-day mean along-track orbit position with a precision of 2–3 mm (Table 5).

## 6 Time bias estimates for Jason, T/P, and ENVISAT orbits

The DORIS time biases estimated over the Jason/TOPEX 10-day orbits and the ENVISAT 7-day orbits are evaluated in this section. Comparing time bias estimates performed using Jason JGM-3 (Tapley et al. 1996) orbits computed at several ACs (Fig. 3), three observations can be made:

1. All the GPS-based orbit estimates are remarkably similar for orbits produced at either GSFC or JPL
2. The GPS-based orbit estimates are similar to the GSFC SLR+DORIS estimates
3. The CNES SLR+DORIS orbit-based estimates differ from the others and are closer to zero

The Jason GPS-based orbits are the most accurate (Luthcke et al. 2003; Haines et al. 2004) and provide the best reference for estimating the DORIS time bias (the cycle 28 GPS-only anomaly seen in Fig. 3 reflects the effect of two 18-h GPS data gaps, October 14 and 15, 2002). The close similarity in the time bias estimates indicates there are no significant mean differences between orbits produced at GSFC or JPL. The small differences between the GPS GSFC/JPL solutions ( $0.46\mu\text{s}$  RMS) are likely due to orbit error, suggesting that the GPS-based orbit error contribution is at the same level as the DORIS resolution precision. This comparison also indicates that the effect of any possible inconsistency in the GPS reference frame realizations between GSFC and JPL cannot cause more than a  $0.4 - 0.5\mu\text{s}$  contribution to the estimated time bias.

The GSFC SLR+DORIS dynamic orbits are determined simultaneously estimating the DORIS time-tag, and are therefore referenced to SLR time. The RMS difference between DORIS time biases estimated with the SLR+DORIS and the GPS orbits is  $1.24\mu\text{s}$  over the 37 cycles and is likely due to a mean along-track orbit error. It was demonstrated (Sect. 5) there is no time offset between SLR and GPS time. Considering the  $0.3-0.4\mu\text{s}$  DORIS precision for resolving a time bias, the  $1-2\mu\text{s}$  contribution of orbit error appears to be the limiting factor in accuracy for estimating the DORIS time bias.

During the calibration/validation phase, the DORIS/Jason time-tag accuracy had been estimated to be better than  $2\mu\text{s}$  based on a direct comparison with GPS/Jason time over a span of 3.5 days (Bonhoure 2002). Those 3.5 days of comparison show a mean DORIS time error of  $-1.036 \pm 0.965\mu\text{s}$ , in contrast to the mean  $\delta\tilde{T}$  of  $-6.017 \pm 2.054\mu\text{s}$  computed over 37 cycles using GSFC GPS orbits, and  $-6.398 \pm 2.410\mu\text{s}$  using the JPL GPS orbits. A more recent analysis (Jayles et al. in press) leads to an even better agreement between DORIS and GPS time on Jason (less than  $1\mu\text{s}$ ). This direct comparison between DORIS and GPS on Jason shows that the

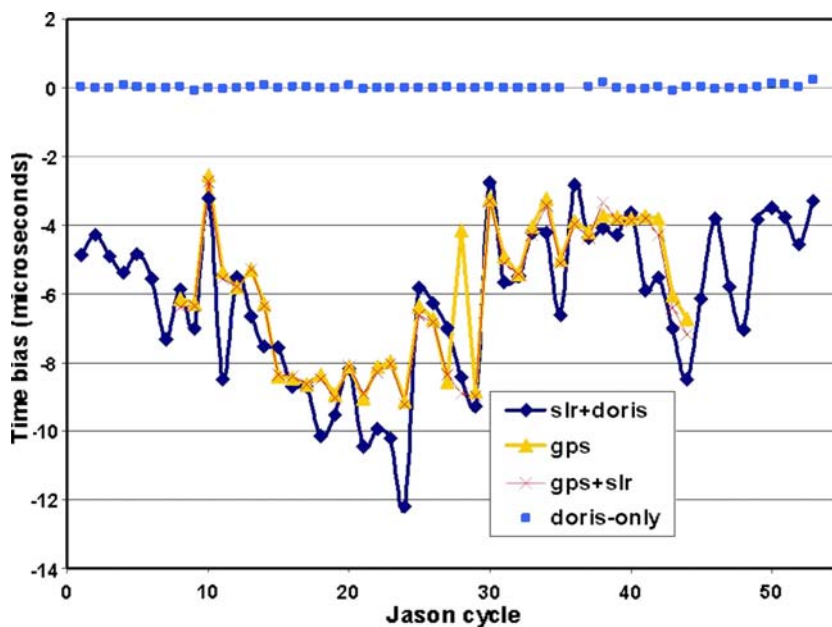


Fig. 1 DORIS time bias estimates with GSFC Jason JGM-3 orbits referencing SLR, GPS, and DORIS time

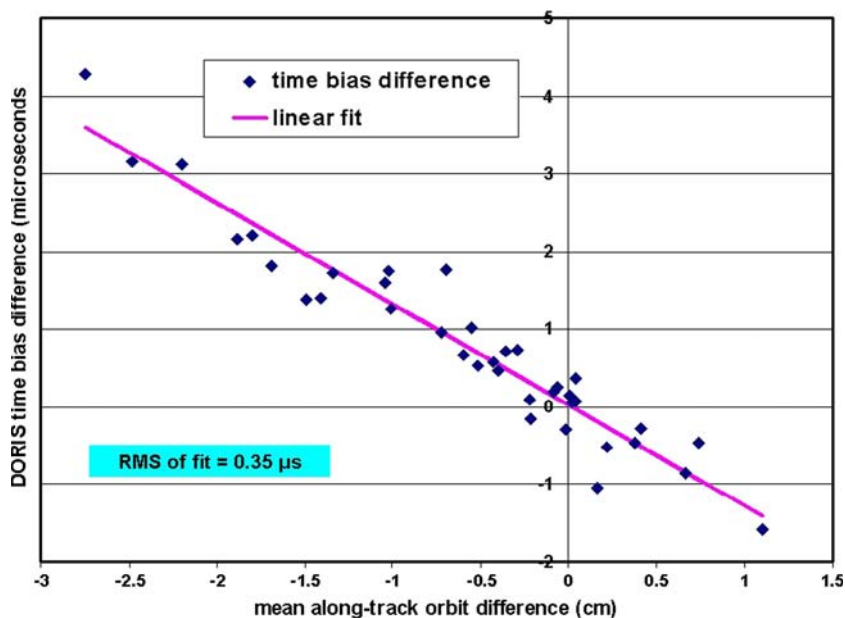


Fig. 2 GPS – SLR+DORIS time bias difference by orbit difference (Jason cycles 8 to 44)

Table 5 Linear regression of Jason GPS-SLR+DORIS orbit and time bias differences

| Independent variable  | Data points | Intercept  |       | Slope         |       | Correlation coefficient | RMS fit    |
|-----------------------|-------------|------------|-------|---------------|-------|-------------------------|------------|
|                       |             | Estimate   | Error | Estimate      | Error |                         |            |
| Time bias differences | 37          | 0.02 (μs)  | 0.07  | -1.30 (μs/cm) | 0.06  | 0.960                   | 0.345 (μs) |
| Orbit differences     | 37          | -0.03 (cm) | 0.05  | -0.71 (cm/μs) | 0.03  | 0.960                   | 0.255 (cm) |

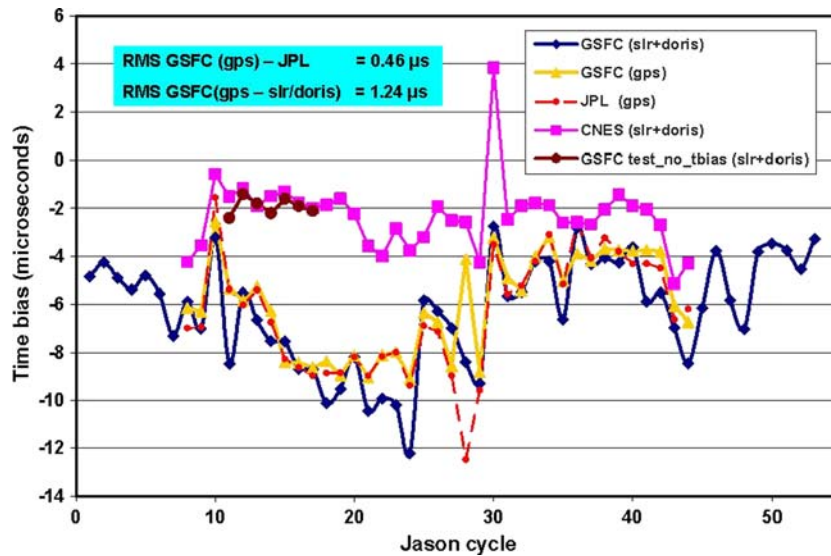


Fig. 3 DORIS time bias estimated over Jason JGM-3 orbits computed at different ACs

relation between DORIS time and TAI is known to micro-second accuracy.

The higher bias measured in orbital tests is therefore an indication that the on-board time of beginning of count may not exactly be what is assumed, and that a possibly erroneous DORIS measurement start time may be the cause of the time bias measured in the orbital tests. An investigation is under way with the instrument manufacturer to measure delays between the time base used for pseudorange measurements and the one used for Doppler measurements (P. Sengenès, private communication).

The final CNES SLR+DORIS orbits show time biases with much smaller deviations from zero (Fig. 3). On average, the  $-3.7 \pm 2.0 \mu\text{s}$  CNES value is about half the GSFC SLR+DORIS value of  $-6.8 \pm 2.4 \mu\text{s}$ . Since the CNES does not estimate a DORIS time bias in the orbit solution, the CNES orbits combine both DORIS and SLR time-scales according to data weights. It appears that the resulting time-scale is somewhere halfway between DORIS and SLR time.

In a test, “test\_no\_tbias”, several SLR+DORIS orbits were computed at GSFC without estimating a time bias in the orbit solution and also decreasing the DORIS sigma weight from 2 to 1 mm/s. The “test\_no\_tbias” POD strategy corresponds to one used for the CNES final orbits (Nouel et al. 1994), and explains the estimated time bias difference seen with the final CNES orbits (Fig. 3). The  $0.35 \mu\text{s}$  RMS difference between the time biases indicates that other than the effect of modeling/not modeling the DORIS time bias, there are no significant mean along-track differences between orbits produced at GSFC or CNES. It is important to note that absorbing such a small time bias does not affect radial orbit accuracy (Table 2). This test also indicates that the effect of any possible inconsistency in the SLR/DORIS reference frame realizations between GSFC and CNES cannot cause more than a  $0.3\text{--}0.4 \mu\text{s}$  contribution to the estimated time bias.

Figure 4 shows DORIS time biases estimated in SLR+DORIS solutions for T/P (cycles 340–446), Jason-1 (cycles 1–135), and ENVISAT (June 16, 2002 – January 1, 2005). Each of the time bias time-series, to some degree, indicate a linear trend with a very small periodic term. Spectral analysis does not reveal any significant signals, showing only a few small (10–12% variance) terms.

Although there is no correlation between the time series in Fig. 4, the means and standard deviations for the three satellites are remarkably similar. Dominance of the  $\delta T_{\text{polynomial}}$  component in the time bias estimate (Eq. 3), would imply that each of the on-board DORIS clocks is in error on average by about  $-7 \mu\text{s}$ , which hardly seems likely. The similarity of the means and standard deviations (Fig. 4) would rather suggest the error source is somehow common to all three satellites. Our analysis is limited towards resolving this issue, and so the DORIS time error source remains of unknown origin.

In a study to derive the DORIS antenna phase maps from DORIS residuals for the DORIS tracked satellites, antenna map patterns were observed which suggest the presence of an  $8 \mu\text{s}$  DORIS time bias in the SPOT data (Willis et al. 2005b). This not only corresponds in magnitude to the biases estimated in our analysis for the T/P, Jason, and ENVISAT satellites, but also suggests that station positions and other geodetic parameters recovered using DORIS data may be sensitive to this effect as well.

Considering a potential progressive degradation of the Jason DORIS oscillator due to irradiation (Willis et al. 2004; Lemoine and Capdeville 2006), the absence of any trend in the estimated Jason time bias time-series (Fig. 4) suggests the estimated time bias is not sensitive to this effect. Supporting this, and further suggesting that the  $\delta T_{\text{polynomial}}$  component (Eq. 3) does not dominate the estimated time bias, Fig. 4 shows the continuity of the estimated Jason time-bias series is preserved, and not broken over cycle 92 (modified Julian

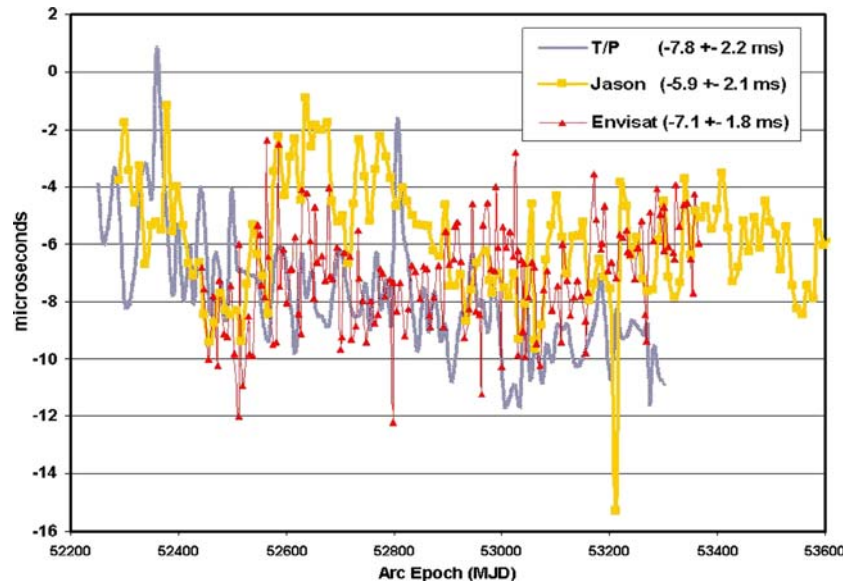


Fig. 4 DORIS time biases estimated using T/P, Jason, and ENVISAT SLR+DORIS orbits

day 53191) when the DORIS oscillators and instruments were switched.

Figure 5 offers a case study of the DORIS time biases for T/P over most of its mission, from the first cycle processed with JGM-3 (degree and order  $70 \times 70$ ) in June 1995 (cycle 93) (Marshall et al. 1995), through November 2004 (cycle 446), when the DORIS system on T/P ceased operations. The time biases are estimated with the SLR+DORIS orbit solution using the modeling from Marshall et al. (1995). The first of the two time-series shown in Fig. 5 was estimated in the GSFC POD Production System (PODPS) determination of the orbit using the JGM-3 gravity field model (Marshall et al. 1995; Tapley et al. 1996).

The second time-series was recently estimated at GSFC with re-imported DORIS data and using the GGM02C gravity field model (degree and order  $70 \times 70$ ), a more recent gravity model derived from more than a year of GRACE data (Tapley et al. 2005). Having 0.98 correlation, the two series show the same picture. The differences between the two are due to differences in the orbits, and in some cases such as for cycle 221, re-processed DORIS data. The RMS difference between the two series (excluding cycle 221) is  $1.6 \mu\text{s}$ , and is consistent with the Jason  $1\text{--}2 \mu\text{s}$  level of dynamic orbit error.

The behavior of the T/P DORIS time bias series (Fig. 5) can be chronologically grouped into three categories, which respectively end with cycles 231, 320, and 446. The demarcation cycles coincide with or are close to the event cycles shown in Fig. 5: switching from nominal to backup DORIS receiver (cycle 231), and Jason launch (cycle 340). An intentional  $6 \mu\text{s}$  offset was applied in the CNES preprocessing to measurements of the nominal receiver up to cycle 231: this largely explains the 4-cm bias until cycle 231, and the nearly  $6 \mu\text{s}$  jump around cycle 231 when the nominal receiver failed and was replaced by the back-up one. With no bias applied,

the plot shows a  $-0.8 \mu\text{s}$  bias average over cycles 232–320. The behavior since cycle 320 is unexplained.

In summary, the DORIS time bias estimated over 10 days, and its components (Eq. 3) can be assigned the following values based on our analysis:

$$\begin{aligned} \delta \ddot{T} &= 5 - 10 \mu\text{s} \\ \delta T_{\text{polynomial}} &= 1 \mu\text{s} \\ \delta T_{\text{orbit}} &= 1 - 2 \mu\text{s} \\ \delta T_{\text{noise}} &= 0.3 - 0.4 \mu\text{s} \\ \delta T_{\text{unknown}} &= 5 - 10 \mu\text{s} \end{aligned}$$

## 7 Time bias estimates over shorter time scales

The DORIS time-tag stability over a 10-day period is addressed by correcting satellite clock time with a third-order polynomial estimated over the same 10-day period (Eq. 2). The DORIS USOs provide a clock stability of about  $10^{-13}$  per pass or about 0.5 ns per 14 min (Brunet et al. 1995; Candelier et al. 2003). This ensures a Doppler precision of better than 0.3 mm/s. However, this same level of clock stability can lead to phase-range-like measurement errors of about 15 cm over a pass. The difference is that Doppler precision depends on stability in frequency over the pass, which is less demanding than clock stability required by the integrated phase measurement.

It has been shown in Table 5 that the DORIS time bias can be recovered with a relative accuracy of  $0.35 \mu\text{s}$  over a 10 day span. Given this level of precision for a DORIS time bias estimated over 10 days, perhaps biases estimated over more frequent intervals will be sufficiently accurate to shed some light on shorter-term stability of DORIS time? This should show the limits of the polynomial modeling over 10 days.



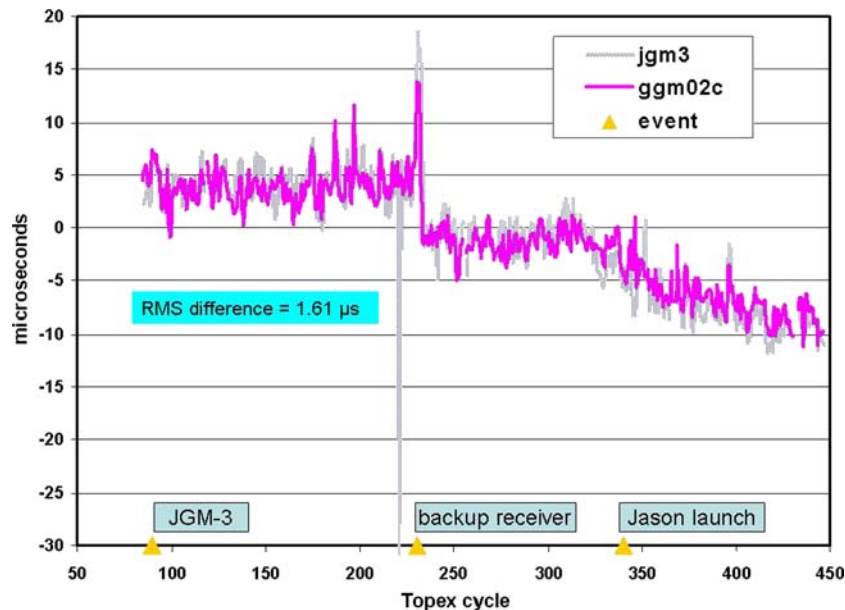


Fig. 5 DORIS time biases estimated with T/P GSFC SLR+DORIS 10-day orbits

However, how stable is the orbit reference over shorter periods of time?

For this test, Jason cycle 12 was selected to ensure the time bias estimates are supported by sufficient DORIS tracking down to 1-h intervals. The DORIS time biases were estimated, as described in Sect. 4, over spans of 10 days, 24, 12, 2, and 1 h, and a DORIS data sigma weight of 0.7 mm/s was applied to calibrate the formal error of a bias to about  $0.3 \mu\text{s}$  when estimated over 10 days. Time biases were estimated using both GSFC GPS reduced-dynamic and SLR+DORIS dynamic JGM-3 orbits (Table 4).

The results (Table 6) demonstrate that as biases are estimated over shorter intervals, the perturbations significantly increase about a mean that stays the same. With the  $-6 \mu\text{s}$  mean removed, the perturbations seem much too large to reflect only fluctuations in the true DORIS time-tag with respect to the modeled polynomial time-tag, and most likely largely represent orbit error, which begins to dominate the estimates over the shorter intervals.

In fact the  $8 \mu\text{s}$  (5 cm) RMS difference between the time biases estimated over 1-h intervals with GPS and SLR+DORIS orbits (Table 6) corresponds well to the 6 cm RMS along-track orbit difference and lends support to the orbit error hypothesis. However, since the  $8 \mu\text{s}$  RMS difference between the time biases is less than either the RMS of the GPS or SLR+DORIS time bias perturbations alone, this indicates to some extent that both orbits agree on the short time-scale fluctuations of the DORIS time tagging.

## 8 Summary and conclusions

This study has evaluated the DORIS time bias estimated using Jason-1, T/P, and ENVISAT satellite orbits, which

reference GPS and SLR time systems. The study asks what does the estimated DORIS time bias show and with what accuracy? The paper includes descriptions of the DORIS measurement, time-tag processing, expected time-tag error, and time bias estimation. The DORIS time bias estimates are evaluated and compared between orbits computed with two different gravity field models, between orbits computed using SLR+DORIS and GPS tracking, and between orbits computed by the GSFC, JPL, and CNES ACs.

Using the relationship between mean along-track orbit differences and between differences in the estimated time bias values, a DORIS precision of  $0.35 \mu\text{s}$  is determined for resolving time biases over a 10-day span using DORIS data alone. The analysis shows there is no offset between the SLR and GPS time that the orbits reference, whereas a  $5\text{--}10 \mu\text{s}$  systematic offset exists for DORIS time, and that the magnitude of this offset can change slowly with time. Our analysis indicates the estimated time bias largely represents an error in the DORIS time, although the specific source for this error remains to be identified.

Evaluating time bias differences estimated with the GPS reduced-dynamic and SLR+DORIS dynamic orbits, our analysis finds mean along-track dynamic orbit error contributing about  $1\text{--}2 \mu\text{s}$  to the estimated 10-day time bias, which is typically under  $10 \mu\text{s}$  in magnitude. As the time span over which the time bias is estimated is shortened from 10-days, our analysis suggests the presence of short time-scale fluctuations of the DORIS time-tagging, which however are hard to quantify since the effect of orbit error significantly increases over the shorter time-spans.

The effect of a  $5\text{--}10 \mu\text{s}$  DORIS time bias error on radial accuracy is negligible (under  $0.005 \text{ cm}$  for T/P). However, the effect of such a small but systematic error may not be negligible for the recovery of geodetic parameters using DORIS

**Table 6** DORIS time biases estimated over several spans using Jason cycle-12 orbit

| Time bias span | Number time biases per arc | Calibrated formal error ( $\mu\text{s}$ ) |              | GPS orbit time bias ( $\mu\text{s}$ ) |              | SLR+DORIS orbit time bias ( $\mu\text{s}$ ) |              | GPS – SLR+DORIS time bias ( $\mu\text{s}$ ) |              |
|----------------|----------------------------|---|--------------|---------------------------------------|--------------|---|--------------|---|--------------|
|                |                            | Mean                                      | Standard dev | Mean                                  | Standard dev | Mean  | Standard dev | Mean  | Standard dev |
| 10 days        | 1                          | 0.332                                     | –            | –5.808                                | –            | –5.516                                      | –            | –0.292                                      | –            |
| 24 h           | 10                         | 1.054                                     | 0.022        | –5.825                                | 1.725        | –5.584                                      | 1.464        | –0.241                                      | 1.874        |
| 12 h           | 20                         | 1.493                                     | 0.045        | –5.906                                | 2.251        | –5.699                                      | 2.159        | –0.206                                      | 2.198        |
| 02 h           | 119                        | 3.790                                     | 0.436        | –6.041                                | 7.388        | –5.913                                      | 8.467        | –0.128                                      | 7.251        |
| 01 h           | 239                        | 5.787                                     | 1.316        | –5.743                                | 10.362       | –5.693                                      | 11.555       | –0.050                                      | 8.153        |

data. It would be interesting to see whether the application of our estimated time biases can bring the DORIS station solution closer to ITRF2000, and if any such systematic station position differences can be used as a signature to identify the presence of a DORIS time bias in the SPOT satellite data.

**Acknowledgments** The authors acknowledge the National Aeronautics and Space Administration and Centre National d'Etudes Spatiales physical oceanography programs, and the TOPEX/Poseidon and Jason-1 projects for their support.

## References

- Altamimi Z, Sillard P, Boucher C (2002) ITRF2000: a new release of the International Terrestrial Reference Frame for earth science applications. *J Geophys Res* 107(B10):2214, DOI 10.1029/2001JB000561
- Berthias JP (2002) CNES Processing Strategy at the Service d'Orbitographie DORIS. In: Proceedings of the IDS Analysis Workshop, Biarritz ([http://ids.cls.fr/html/report/ids\\_workshop\\_2002/JPB\\_processing\\_IDS2002.pdf](http://ids.cls.fr/html/report/ids_workshop_2002/JPB_processing_IDS2002.pdf))
- Bonhoure B (2002) DORIS performances. In: Proceedings of the ENVISAT validation workshop presentation, Dec 9–13, European Space Research INstitute (ESRIN), Frascati ([http://ids.cls.fr/html/report/publications/ENVISAT\\_Validation\\_Workshop\\_2002\\_DORIS\\_BB.pdf](http://ids.cls.fr/html/report/publications/ENVISAT_Validation_Workshop_2002_DORIS_BB.pdf))
- Brunet M, Auriol A, Agnieray P, Nouel F (1995) DORIS precise orbit determination and localization – system description and USOs performances. In: Proceedings of the 1995 IEEE international frequency control symposium, pp 122–132 (<http://ieeexplore.ieee.org/iel2/3499/10330/00483892.pdf?arnumber=483892>)
- Candelier V, Canzian P, Lamboley J, Brunet M, Santarelli G (2003) Space qualified 5 MHz ultra stable oscillators. In: Proceedings of the 2003 IEEE international frequency control symposium and PDA exhibition, pp 575–582 (<http://ieeexplore.ieee.org/iel5/8990/28531/01275155.pdf?arnumber=1275155>)
- Escudier P, Auriol A, Coutin-Faye S, Costes M (1998) DORIS activities and components. In: Proceedings of the DORIS Days, Centre National d'Etudes Spatiales (CNES), Toulouse
- Haines B, Bar-Sever Y, Bertiger W, Desai S, Munson T, Willis P (2003) Precise orbit determination for Jason-1: GPS and the 1-cm solution. Jason-1 Science Working Team (SWT) Arles (<http://www.jason.oceanobs.com/documents/swt/posters2003/haines2.pdf>)
- Haines B, Bar-Sever Y, Bertiger W, Desai S, Willis P (2004) One-centimeter Orbit Determination for Jason-1: New GPS-based Strategies. *Marine Geodesy*, 27(1–2):299–331: DOI 10.1080/01490410490465300
- Hutsell S, Forsyth M, McFarland CB (2002) One-Way GPS Time Transfer: 2002 Performance. Proc 34th Annual Time and Time Interval (PTTI) Meeting Proceedings, Dec 3–5, Reston (<http://tycho.usno.navy.mil/ptti/ptti2002/paper6.pdf>)
- Jayles CB, Nhun-Fat, Tourain C (2006). DORIS system description and control of the signal integrity. *J Geod* (in press), DOI 10.1007/s00190-006-0046-8
- Lemoine JM, Capdeville H (2006) Corrective model for Jason-1 DORIS Doppler data related to the South Atlantic Anomaly, *J Geod* (in press)
- Luthcke SB, Zelensky NP, Rowlands DD, Lemoine FG, Williams TA (2003) The 1-centimeter orbit: Jason-1 precision orbit determination using GPS, SLR, DORIS and altimeter data. *Mar Geod* 26(3–4):399–421, DOI 10.1080/01490410390256727
- Marshall JA, Zelensky NP, Luthcke SB, Rachlin KE, Williamson RG (1995) The temporal and spatial characteristics of TOPEX/Poseidon radial orbit error *J Geophys Res* 100(C12):25331–25352
- McCarthy DD, Petit G (Eds.) (2003) IERS Conventions 2003, IERS Tech. Note 32, Verlag des Bundesamts für Kartographie und Geodäsie, Frankfurt-am-Main
- Menard Y, Fu LL, Escudier P, Parisot F, Perbos J, Vincent P, Desai S, Haines B, Kuntzmann G (2003) The Jason-1 mission. *Mar Geod* 26(3–4):131–146, DOI 10.1080/01490410390256736
- Nouel F, Berthias JP, Deleuze M, Guitart A, Laudet P, Piuze A, Pradines D, Valorge C, Dejoie C, Susini MF, Taburiau D (1994) Precise Centre National d'Etudes Spatiales orbits for TOPEX/POSEIDON: is reaching 2 cm still a challenge?. TOPEX/Poseidon mission overview. *J Geophys Res* 99(C12):24405–24420
- Pavlis DE (2006) GEODYN operations manuals, 5 volumes, Contractor report. SGT-Inc, Greenbelt
- Pearlman MR, Degnan JJ, Bosworth JM (2002) The International Laser Ranging Service. *Adv Space Res* 30(2):135–143
- Tapley BD, Watkins MM, Ries JC, Davis GW, Eanes RJ, Poole SR, Rim HJ, Schutz BE, Shum CK, Nerem RS, Lerch FJ, Marshall JA, Klosko SM, Pavlis NK, Williamson RG (1996) The JGM-3 geopotential model. *J Geophys Res* 101(B12):28029–28049
- Tapley BD, Ries J, Bettadpur S, Chambers D, Cheng M, Condi F, Gunter G, Kang Z, Nagel P, Pastor R, Pekker T, Poole S, Wang F (2005) GGM02 – an improved Earth gravity model from GRACE. *J Geod* 79(8):467–478, DOI 10.1007/s00190-005-0480-z
- Tavernier G, Granier JP, Jayles C, Sengenès P, Roza F (2003) The current evolutions of the DORIS system. *Adv Space Res* 31(8):1947–1952, DOI 10.1016/S0273-1177(03)00155-8.
- Tavernier G, Fagard H, Feissel-Vernier M, Lemoine F, Noll C, Ries J, Soudarin L, Willis P (2005) The International DORIS Service (IDS). *Adv Space Res* 36(3): 333–341, DOI 10.1016/j.asr.2005.03.102.
- Willis P, Haines B, Berthias JP, Sengenès P, Le Mouél JL (2004) Behavior of the DORIS/Jason oscillator over the South Atlantic Anomaly. *CR Geosci* 336(9):839–846, DOI 10.1016/j.crte.2004.01.004.
- Willis P, Ries JC (2005) Defining a DORIS core network for Jason-1 precise orbit determination based on ITRF2000, Methods and realizations. *J Geod* 79(6–7):370–378, DOI 10.1007/s00190-005-0475-9
- Willis P, Boucher C, Fagard H, Altamimi Z (2005a) Geodetic applications of the DORIS system at the French 'Institut géographique national'. *CR Geosci* 337(7): 653–662, DOI 10.1016/j.crte.2005.03.002
- Willis P, Desai SD, Bertiger WI, Haines BJ, Auriol A (2005b) DORIS satellite antenna maps derived from long-term residuals time series. *Adv Space Res* 36(3):486–497, DOI 10.1016/j.asr.2005.03.095.